A Generalized Fuzzy Mathematical Morphology and its Application in Robust 2D and 3D Object Representation

Vassilios Chatzis and Ioannis Pitas

The authors are with the Department of Informatics, Aristotle University of Thessaloniki. Corresponding author: Ioannis Pitas, University of Thessaloniki, GR-54006 Thessaloniki, GREECE, phone,fax: +30-31-996304, e-mails: [chatzis,pitas]@zeus.csd.auth.gr, EDICS number: IP 1.8 (Image Representation).

Abstract

In this paper, the Generalized Fuzzy Mathematical Morphology (GFMM) is proposed, based on a novel definition of a Fuzzy Inclusion Indicator (FII). A FII is a measure of the inclusion of a fuzzy set into another, that is proposed to be a fuzzy set. It is proven that the FII obeys a set of axioms, which are proposed to be extensions of the known axioms that any inclusion indicator should obey, and which correspond to the desirable properties of any mathematical morphology. The GFMM provides a very powerful and flexible tool for morphological operations. The Binary and Grayscale mathematical morphologies can be considered as special cases of the proposed GFMM. An application for robust skeletonization and shape decomposition of 2D and 3D objects is presented. Simulation examples show that the reconstruction of objects from their skeletal subsets, that can be achieved by using the GFMM is better than by using the BMM. Furthermore, the use of the GFMM for skeletonization and shape decomposition preserves the shape and the location of the skeletal subsets and spines.

I. Introduction

Mathematical morphology is a very rich and powerful tool used for the representation and analysis of binary and grayscale images [1]-[6]. The morphological image representation has been used for the description of the geometrical characteristics of image objects as well as for binary image compression. The morphological skeleton and the morphological shape decomposition are the very popular methods for morphological shape representation [7], [8]. Although several comparative studies and properties analysis can be found in the literature [7]-[10] the main disadvantage of both methods is the lack of robustness especially in impulsive noise, something that can be considered as a general characteristic of all the morphological operations [11].

Several efforts have been done to reduce the sensitivity of morphological operations in impulses. Soft morphological operations have been proposed in [12], which can restrict the problem in some cases. The properties of soft mathematical morphology have been also investigated [13], [14]. Fuzzy morphological operations have also been proposed and investigated rather recently [15]-[20], but still the fuzzy and soft morphologies are not efficient in binary object representation, since skeletonization and shape decomposition have strong dependency on the presence of outliers alike the classical Binary Mathematical Morphology.

In this paper a novel Generalized Fuzzy Mathematical Morphology (GFMM) is proposed. The GFMM is based on a Fuzzy Inclusion Indicator (FII), a measure of the inclusion of a fuzzy set into another, that is proposed to be a fuzzy set. It is proven that the FII obeys a set of axioms, which are proposed to be extensions of the known axioms that any inclusion indicator should obey, and correspond to desirable characteristics that any mathematical morphology should have. The Binary and Grayscale mathematical morphologies can be considered as special cases of the proposed GFMM. The GFMM provides a very powerful and flexible tool. In this paper an application for robust skeletonization and shape decomposition of 2D and 3D objects is presented.

The paper has the following structure. In section II the fuzzy sets relations and operations are presented in brief. In section III the Fuzzy Inclusion Indicator (FII) is defined grounded on an axiomatic basis that is also commented. The FII is also compared with other inclusion indices. In section IV the Generalized Fuzzy Mathematical Morphology is defined. The basic morphological operations are presented and the compatibility with Binary and Grayscale mathematical morphologies is shown. The flexibility of the GFMM is presented by using an example where the property of robustness is considered desirable. Simulation results on the use of the GFMM for robust skeletonization and shape decomposition of images and volumes are presented in section V. Conclusions are drawn in section VI. Appendix A includes the proofs of the compliance of the FII on the axioms proposed in section III.

II. Fuzzy Sets and Fuzzy Arithmetic

The notion of a fuzzy set A, introduced primarily in [21], is usually described by its membership function μ_A that maps the universal set U to the interval $[0,1]$:

$$A = \{x, \mu_A(x)\}, \qquad \mu_A : U \to [0,1] \tag{1}$$

The value $\mu_A(x)$ is called the degree of membership of the point x to the set A. A more effective representation of a fuzzy set A is the union of its α-cuts A^α, which are defined as the crisp sets of the points $x : \mu_A(x) \geq \alpha$:

$$A = \bigcup_\alpha A^\alpha \tag{2}$$

The classical relations (subset $\subset$) and operations (union $\cup$ and intersection $\cap$) have been extended to fuzzy sets. Although several definitions can been found in the literature, the most frequently used are the classical definitions that follow. Let A, B be two fuzzy sets with membership values μ_A, μ_B, the union and intersection of A, B are the fuzzy sets $A \cup B$ and $A \cap B$

with membership functions $\mu_{A\cup B}$ and $\mu_{A\cap B}$ given by:

$$\mu_{A\cup B}(x) = \max\{\mu_A(x), \mu_B(x)\} \tag{3}$$

$$\mu_{A\cap B}(x) = \min\{\mu_A(x), \mu_B(x)\} \tag{4}$$

A fuzzy set A is considered subset of the fuzzy set B if and only if the membership degree $\mu_A(x)$ of A is less than or equal to the membership degree $\mu_B(x)$ of B for all x:

$$A \subset B \Leftrightarrow \mu_A(x) \leq \mu_B(x), \quad \forall x \tag{5}$$

From equations (3),(4) and (5) the following equivalent expressions using the α-cuts, can be derived:

$$(\bigcup_i B_i)^\alpha = \bigcup_i (B_i^\alpha) \tag{6}$$

$$(\bigcap_i B_i)^\alpha = \bigcap_i (B_i^\alpha) \tag{7}$$

$$A \subset B \Rightarrow A^\alpha \subseteq B^\alpha, \quad \forall \alpha \in [0,1] \tag{8}$$

The complement of a fuzzy set A is usually defined as the fuzzy set A^c with membership function:

$$\mu_{A^c}(x) = 1 - \mu_A(x) \tag{9}$$

The translation of a fuzzy set A by a crisp vector v is the fuzzy set $T(A;v)$ with membership function:

$$\mu_{T(A;v)}(x) = \mu_A(x - v) \tag{10}$$

Similarly, the centrally symmetric of a fuzzy set A is the fuzzy set $-A$ with membership function $\mu_{-A}(x) = \mu_A(-x)$.

III. The Fuzzy Inclusion Indicator (FII)

A. Axiomatic basis of the Fuzzy Inclusion Indicator

An *inclusion indicator* or *inclusion grade operator* I measures the belief in the proposition "A is a subset of B", where A, B are fuzzy sets. It has been defined in the literature as a two argument function $I(A, B)$, that maps any couple of fuzzy sets A, B into the interval [0,1], and satisfies a number of axioms (properties) [15], [16], [17]:

- A1: $I(A,B) = 0$ if and only if $\{x : \mu_A(x) = 1\} \cap \{x : \mu_B(x) = 0\} \neq \emptyset$,
- A2: $B \subset C \Rightarrow I(A,B) \leq I(A,C)$,
- A3: $B \subset C \Rightarrow I(C,A) \leq I(B,A)$,
- A4: $I(A,B) = I(T(A;v), T(B;v))\ \forall v$, $I(A,B) = I(-A,-B)$,
- A5: $I(A,B) = I(B^c, A^c)$,
- A6: $I(\bigcup_i B_i, A) = \inf_i I(B_i, A)$,
- A7: $I(A, \bigcap_i B_i) = \inf_i I(A, B_i)$,
- A8: $I(A, \bigcup_i B_i) \geq \sup_i I(A, B_i)$.

Another axiom that has been proposed by [16]:

- A9: $I(A,B) = 1$ if and only if $A \subset B$,

has been found too restrictive since it is not satisfied by most of the inclusion indicators proposed in the literature [15]. The above mentioned axioms are not independent since for example A3 can be derived by applying A5 to A2 and A7 can be derived by applying A5 to A6. Equivalences between these nine axioms and the desired properties of a fuzzy mathematical morphology are extensively quested in [17]. It is just mentioned here that A4 is strongly related with the translation invariance property, A5 with the principle of duality, A1 and A9 lead to the compatibility of the constructed fuzzy mathematical morphology with the binary and grayscale one, A2 and A3 are related with the increasingness (decreasingness) of erosion with respect to the reference (structuring element) set, and A6, A7 and A8 are related with the compatibility with union and intersection in classical morphology.

In the following a generalized fuzzy mathematical morphology (GFMM) will be constructed based on the novel definition of an inclusion indicator as a fuzzy set rather than a number, defined in the interval $[0,1]$. Large membership values strengthen the belief that "A is a subset of B". The use of a fuzzy inclusion indicator in the construction of a fuzzy mathematical morphology removes the paradox that fuzzy mathematical operations on fuzzy signals result to crisp signals.

Definition 1: A *fuzzy inclusion indicator* is any two argument function $\mathbf{I}$, that maps a couple of fuzzy sets A, B into another fuzzy set with domain of definition the interval $[0,1]$, and satisfies the following axioms:

- **A1**: $\mathbf{I}(A,B) = O$ if and only if $\forall \alpha \in [0,1], \{x : \mu_A(x) = \alpha\} \cap \{x : \mu_B(x) = 0\} \neq \emptyset$,
- **A2**: $B \subset C \Rightarrow \mathbf{I}(A,B) \subseteq \mathbf{I}(A,C)$,

- **A3**: $B \subset C \Rightarrow \mathbf{I}(C, A) \subseteq \mathbf{I}(B, A)$,
- **A4**: $\mathbf{I}(A, B) = \mathbf{I}(T(A; v), T(B; v)) \; \forall v$, $\mathbf{I}(A, B) = \mathbf{I}(-A, -B)$,
- **A5**: $\mathbf{I}(\bigcup_i B_i, A) = \bigcap_i \mathbf{I}(B_i, A)$,
- **A6**: $\mathbf{I}(A, \bigcap_i B_i) = \bigcap_i \mathbf{I}(A, B_i)$,
- **A7**: $\mathbf{I}(A, \bigcup_i B_i) \supseteq \bigcup_i \mathbf{I}(A, B_i)$,

where O is the zero fuzzy set with membership function $\mu_O(x) = 0$. These seven axioms **A**1 - **A**7 are extensions of the previously reported axioms A1 - A4 and A6 - A8 that are fundamental for the construction of any fuzzy mathematical morphology. Thus, the GFMM that will be constructed based on these seven axioms will have the desired properties of any mathematical morphology: translation invariance (**A**4), compatibility with the binary and grayscale mathematical morphologies (**A1**), increasingness (decreasingness) of erosion with respect to the reference (structuring element) set (**A2**, **A3**), compatibility with union and intersection in classical morphology (**A5**, **A6**, **A7**). Although the principle of duality will be taken into account in the construction of the GFMM, the axiom A5 was not extended to be included into the axioms that a fuzzy inclusion indicator should obey, since the complementation is a function that changes the membership values of the fuzzy sets in contrast to the other axioms.

B. The Fuzzy Inclusion Indicator definition

The *Extension Principle (EP)* is often used in fuzzy theory to extend mathematical laws of crisp numbers to fuzzy sets [22], [23]. It provides the theoretical warranty that fuzzifying the parameters or arguments of a function results in computable fuzzy sets. Let $X_1, X_2, \ldots, X_n$ be n fuzzy sets and $y = f(x_1, x_2, \ldots, x_n)$ be a crisp function. Then, the extension principle transfers the fuzziness of $X_1, X_2, \ldots, X_n$ through the function f to a fuzzy set $Y = \{y, \mu_Y(y)\}$ where:

$$\mu_Y(y) = \begin{cases} 0 & \text{if } f^{-1}(y) = \emptyset \\ sup_{(x_1, x_2, \ldots, x_n) \in f^{-1}(y)} min\{\mu_{X_1}, \mu_{X_2}, \ldots, \mu_{X_n}\} & \text{if } f^{-1}(y) \neq \emptyset \end{cases} \tag{11}$$

Although the inclusion indicator function does not have a similar function in crisp arithmetic, an EP-like operation has been proposed in [24], [25] to define the compatibility index τ as a fuzzy inclusion index of a fuzzy set A with respect to another fuzzy set B:

$$\mu_\tau(u) = \sup_{x : \mu_A(x) = u} \mu_B(x) \qquad \forall u \in [0, 1] \tag{12}$$

However, since the compatibility index applies a $T - conorm$ (sup) operator, it cannot be used for the definition of an erosion operation. We can reach the same conclusion, by observing that the compatibility index does not satisfy the axioms **A5** and **A6**.

In this paper a novel fuzzy inclusion indicator is proposed, by applying a $T - norm$ (inf) operator on the EP-like operation (12) as follows. Let A, B be two fuzzy sets. A fuzzy inclusion indicator $\mathbf{I}(A, B)$ is defined as a fuzzy set with membership function:

$$\mu_{\mathbf{I}(A,B)}(u) = \inf_{x:\mu_A(x)=u} \mu_B(x) \qquad \forall u \in [0,1] \tag{13}$$

The proposed fuzzy inclusion indicator (13) satisfies the axioms **A1** - **A7**. The proofs are presented in Appendix A.

The main difference between the proposed fuzzy inclusion indicator and other known indicators is that the proposed indicator is generally a fuzzy set defined in $[0, 1]$ instead of a crisp number in $[0, 1]$. Although this characteristic provides the propagation of fuzziness through the inclusion operation, a crisp value could be desirable in some cases. Then, a defuzzification process should be followed symbolized as $D(\mathbf{I})$. The resulting crisp value of inclusion I should vary from 0 to 1:

$$I(A, B) = D(\mathbf{I}(A, B)) \tag{14}$$

A variety of defuzzification processes have been proposed in the literature [23], [25], [26]. The most usual ones are the center of gravity method, the center of maxima method and the mean of maxima method as well as generalizations or weighted versions of them.

Some examples of fuzzy inclusion indicators between fuzzy sets, crisp sets and crisp numbers are given in Figure 1. We can observe in Figure 1a that the domain of definition of the inclusion operation is assigned by the included set A. Subsets of A, defined from its membership function through the equation $x : \mu_A(x) = \alpha$, provide the subdomains where the inf operator is applied on the values of the membership function $\mu_B(x)$ of the reference set B. The correspondence of the values α to the values $\inf\{\mu_B(x)\}$ constructs the fuzzy set that is the fuzzy inclusion indicator $\mathbf{I}(A, B)$. It is also shown in Figure 1b that the fuzzy inclusion of a crisp set into a fuzzy set is the minimum membership value of B in the crisp set, corresponded to the unity, and that the fuzzy inclusion of a fuzzy set into a crisp set is generally a crisp set in $[0, 1]$. In Figure 1c it is shown that the inclusion of a crisp value x into a fuzzy set B is the membership value $\mu_B(x)$, corresponding to unity. It is also easy to show that the fuzzy inclusion of a crisp set or a crisp value into a crisp set are extensions of classical set theory relations.

C. Comparison with other inclusion indices

In [17] a fuzzy mathematical morphology is defined based on the indicator:

$$I_1(A,B) = \int_0^1 \inf_{x \in A^\alpha} \mu_B(x) d\alpha. \tag{15}$$

The indicator (15) is similar to the proposed fuzzy inclusion indicator (13), since it applies an inf operator on values of the membership function of the fuzzy set B that belong in subsets of the support of A. The integral can be considered as a special case of the defuzzification process of the fuzzy indicator. The main difference of the two indicators is that the subsets in (15) are the α-cuts of the fuzzy set A while the subsets in (13) are defined as the subsets of the support of A where $\mu_A(x) = \alpha$, a process that is similar to the extension principle one. In general, the indicator (15) satisfies axioms A6 and A7 like inequalities. Thus, the associated erosion definition is not an erosion according to the general definition of [27].

Several other inclusion indicators have been proposed in the literature in the last decade and have been successively used for the definition of fuzzy mathematical morphologies. A family of λ functions, which satisfy special characteristics, has been proposed in [16] to define a family of inclusion indicators as:

$$I_2(A,B) = \inf_x \min\{1, \lambda(\mu_A(x)) + \lambda(1 - \mu_B(x))\} \tag{16}$$

This indicator satisfies the eight axioms A1-A8 and is studied in detail in [16], [17]. Another inclusion indicator that leads to fuzzy morphological operations proposed in [28] is:

$$I_3(A,B) = \inf_x \max\{\mu_B(x), 1 - \mu_A(x)\} \tag{17}$$

which has been used especially in the study of fuzzy convexity. Other inclusion indicator indices, properties and comparative studies can been found in [15], [16], [17], [19], [29].

IV. The Generalized Fuzzy Mathematical Morphology (GFMM)

A. Definition of the basic morphological operations

Based on the previously defined fuzzy inclusion indicator (13), the Generalized Fuzzy Mathematical Morphology framework will be constructed. In the following, the four basic operations of any morphology, erosion, dilation, opening and closing will be defined. Let A, B be two fuzzy sets. The erosion of the fuzzy set A by the fuzzy set B, which will be called *fuzzy structuring* *element* subsequently, is defined as the fuzzy set $\mathcal{E}(A,B)$ having membership function given by:

$$\mu_{\mathcal{E}(A,B)}(x) = \mu_{\mathbf{I}(T(B;x),A)}(D(\mathbf{I}(T(B;x),A)) \tag{18}$$

where $\mathbf{I}$ denotes the fuzzy inclusion indicator and D is a defuzzification procedure. The dilation $\mathcal{D}(A,B)$ is then defined to obey to the duality principle:

$$\mathcal{D}(A,B) = \mathcal{E}(A^c, -B)^c \tag{19}$$

where $-B$ denotes the centrally symmetric of the fuzzy structuring element B and A^c the complement of the fuzzy set A as in (9). Opening and closing are defined in terms of erosion and dilation:

$$\mathcal{O}(A,B) = \mathcal{D}(\mathcal{E}(A,B),B) \tag{20}$$

$$\mathcal{C}(A,B) = \mathcal{E}(\mathcal{D}(A,-B),-B). \tag{21}$$

It can be observed in (18) that the membership value of the eroded set is the value of the fuzzy inclusion indicator membership function, at the point resulting from the defuzzification procedure of the fuzzy inclusion indicator. Since the fuzzy inclusion indicator membership function takes its values from the membership function of the reference set, the eroded set takes also values coming from the reference set. The neighbor of the reference set that takes part in the erosion procedure is defined by the fuzzy structuring element. The above mentioned characteristics are similar with the classical morphological ones. The fuzziness of the structuring element forms sets with equal membership, which are responsible for the topological characteristics and special features of the corresponding morphological operations.

B. Compatibility with classical mathematical morphologies

In the following it will be shown that the classical Binary Mathematical Morphology (BMM) can be considered as a special case of the proposed Generalized Fuzzy Mathematical Morphology. Let A_c, B_c be two classical sets defined in a subset of R^n and any $x \in A_c$ correspond to a value in $\{0,1\}$ through a function $f_{A_c}(x)$. The above sets are considered as a reference and a structuring element set respectively of the classical BMM. In the GFMM framework the two valued reference set A is equivalent to a fuzzy set with a bi-valued membership function $\mu_A(x) = f_{A_c}(x)$. Let also B be a fuzzy set defined in the same domain as the classical set B_c, having a membership value $\mu_B(x) = 1$. For this special case of A, B, the fuzzy inclusion indicator membership function (13) is simplified as follows:

$$\mu_{\mathbf{I}(B,A)}(u) = \begin{cases} 0 & \text{if } \exists x \in B : \mu_A(x) = 0 \\ 1 & \text{otherwise} \end{cases}, u = 1. \tag{22}$$

that is defined only in the set $u = 1$. Then, any defuzzification process in (18) leads to $D = 1$ and the corresponding fuzzy erosion operation is simplified to:

$$\mu_{\mathcal{E}(A,B)}(x) = \begin{cases} 0 & \text{if } \exists x \in T(B;x) : \mu_A(x) = 0 \\ 1 & \text{otherwise} \end{cases} \tag{23}$$

which is equivalent to the definition of the classical binary erosion.

The Grayscale Mathematical Morphology (GMM) assumes that the reference set A_c takes values, through a function $f_{A_c}(x)$, in a certain convex set. Normalizing the values of the convex set in $[0,1]$, any membership function of a certain fuzzy set A can substitute the function f. The fuzzy structuring element is defined as in the previous case. For this special case of A, B the fuzzy inclusion indicator membership function (13) is simplified as follows:

$$\mu_{\mathbf{I}(B,A)}(u) = \inf_{x \in B} \mu_A(x) \qquad u = 1 \tag{24}$$

that is defined only in $u = 1$ set. Then, any defuzzification process in (18) leads to $D = 1$ and the corresponding fuzzy erosion operation is simplified to:

$$\mu_{\mathcal{E}(A,B)}(x) = \inf_{x \in T(B;x)} \mu_A(x) \tag{25}$$

which is equivalent to the definition of the classical grayscale erosion. It can be concluded from (23) and (25) that BMM and GMM can be considered as special cases of the proposed GFMM.

C. Properties of the GFMM - Robustness

It was presented in the previous section that, by using a crisp set as a fuzzy structuring element, the GFMM can include the BMM and the GMM as special cases and inherit the properties of the corresponding morphological operations. In the following, it will be shown that the properties of the GFMM can be handled by the membership function of the fuzzy structuring element. The role of the membership function is important during the calculation of the fuzzy inclusion indicator. The membership function of the fuzzy structuring element B defines classical sets of points with equal degree of membership in B. The meaning of the membership equality is that it defines a locus of topological similarity. Then, the inf operation of the inclusion indicator takes place among the points that belong to each classical set of equal membership separately, and the infimum values are used to construct the fuzzy inclusion indicator set. Similarly with the definition of a fuzzy structuring element in other fuzzy mathematical morphologies, the fuzzy structuring element can be separated in two parts, the core where the membership function equals unit, and the fuzziness which is the rest of the element. The core is responsible for the properties which come from the classical morphological operation. The fuzziness of the membership function of the fuzzy structuring element can cause different behavior of the GFMM operations, and a suitable selection of it, can lead to desirable characteristics. An example of a selection that leads to a robust mathematical morphology will be presented in the following.

Let A be a binary 10×10 image with a rectangular object, corrupted by an impulse of zero value in pixel $(4,4)$, shown in Figure 2a. Let B be a fuzzy structuring element with pyramidal membership function defined in a 5×5 classical set, shown in Figure 2b. Since the core set has support area less than a pixel the corresponding classical erosion would leave the image unchanged. The fuzzy inclusion indicators of the translated structuring element $T(B;v)$ in the image A for various translations v are shown in Figure 2c, Figure 2d and Figure 2e. The simplest choice, the center of maxima defuzzification procedure is selected in this example. Each pixel of the eroded image $\mathcal{E}(A,B)$ that is shown in Figure 2f, has been substituted by the maximum value of the fuzzy inclusion indicator membership function. This example emphasizes that a robust morphology in the presence of impulsive noise can be constructed by using a pyramidal fuzzy structuring element. When the core set has area greater than a pixel the robustness is combined with the properties of the classical erosion operation.

V. Application in robust object shape representation

The morphological skeleton and the morphological shape decomposition are popular methods for shape representation. Each method represents an object X as a number of components. Algebraic combinations of the components reconstruct the object. The representation of X using the morphological skeleton is [7]:

$$X = \bigcup_{k=0}^{N} S(k) \oplus kB \tag{26}$$

where the sets $S(k)$ known as *skeletal subsets* are:

$$S(k) = (X \ominus kB) \backslash (X \ominus kB)_B \tag{27}$$

where $\ominus$ and $\oplus$ are morphological erosion and dilation, X_B is the morphological opening of X by B, $X \backslash Y$ is the part of X that does not belong in Y, kB is the kth-order homothetic of B and N is the largest integer such that $X - NB \neq \emptyset$.

The morphological shape decomposition of X is described by [8]:

$$X = \bigcup_{k=0}^{N} L(k) \oplus kB \tag{28}$$

where the sets $L(k)$ known as *spines* are:

$$L(k) = \begin{cases} (X \backslash (\bigcup_{j=k+1}^{N} L(j) \oplus jB)) \ominus kB, & 0 \leq k < N \\ X \ominus NB, & k = N \end{cases} \tag{29}$$

where N is again the largest integer such that $X - NB \neq \emptyset$.

Skeletonization and shape decomposition based on the GFMM morphology can be applied by substituting the classical erosion, dilation and opening operations that are used during their processes, with the corresponding operations of the GFMM defined in (18), (19) and (20). Since X is a binary image, the simplified erosion equation given in (23) can be used. Simplified versions of dilation and opening are derived easily. The fuzzy structuring element was chosen to have a size of 9×9 pixels, a core set of 3×3 pixels where $\mu_B = 1$, and pyramidal fuzziness. Extensive simulations were applied by using two reference images. The first one contains an orthogonal spiral and it is shown in Figures 3a and 5a. The second one contains a puzzle piece and it is shown in Figures 4a and 6a. Each image was contaminated by impulsive (salt and pepper) noise. The noise probability varied from 0.1% to 20%. Since the location of the impulses in respect with the object strongly affects the resulting skeletal subsets and spines, several experiments were performed for the same noise probability.

The skeletonization results are presented in Tables I and II for the *spiral* and the *puzzle* image respectively. The number of the skeletal subsets, the area of the noisy object X' as a percentage of the original, the total area of the skeletal subsets as a percentage of the original, and the area of the reconstructed from the skeletal subsets object $\hat{X}$ as a percentage of the original are presented in the Tables. The representation error is also presented as the sum of the positive error defined as the number of pixels that belongs in X and does not belong in $\hat{X}$, and the negative error defined as the number of pixels that belongs in $\hat{X}$ and does not belong in X. It should be noted that, in order to avoid reconstructing the white impulses on the background, the last step of the reconstruction was omitted. It can be observed that the representation error is always less by using the proposed GFMM than by using BMM. The reconstructed area is also greater in the GFMM case. Generally, the reconstruction of objects from their skeletal subsets, that can be achieved by using the GFMM is better than obtained by using the BMM. However, the most important characteristic of the use of GFMM is the preservation of the shape and the location of the skeletal subsets. An indication of this property is the number of skeletal subsets, presented in Tables I and II. Figures 3 and 4 illustrate the above mentioned property. The original spiral image, the BMM skeleton, the reconstructed from the BMM skeleton object, the GFMM skeleton and the GFMM reconstructed object are shown in Figures 3a to 3e. In Figures 3f to 3o the skeletonization process is applied on the noisy spiral images shown, and the corresponding BMM and GFMM skeletons and reconstructed object are also presented. The corresponding results when skeletonization is applied on the original and two noisy puzzle images are presented in Figure 4.

The shape decomposition results are presented in Tables III and IV for the *spiral* and the *puzzle* image respectively. The number of the spines, the area of the noisy object X', the area of the spines and the area of the reconstructed object as percentages of the original, and the representation error are presented in the Tables. The representation error and the reconstructed area are more or less similar by using the GFMM and the BMM. The shape and the location of the spines are preserved better in the case of GFMM. The number of spines is in most cases closer to the number of the original objects spines by using the GFMM shape decomposition. Figures 5 and 6 illustrate the above mentioned property. The original spiral image, the BMM spines, the reconstructed object from the BMM spines, the GFMM spines and the GFMM reconstructed object are shown in Figures 5a to 5e. In Figures 5f to 5o the shape decomposition process is applied on the noisy spiral images shown, and the corresponding BMM and GFMM skeletons and reconstructed object are also presented. The corresponding results when skeletonization is applied on the original and two noisy puzzle images are presented in Figure 6.

Simulations were also performed on 3D data. The BMM and GFMM skeletonization and shape decomposition were applied on the binary volume of a human body shown in Figures 7a and 8a [30],[31]. Two projections of the morphological skeleton of the body by using either BMM or GFMM are shown in Figures 7b and Figures 7c. Both skeleton and shape decomposition processes were also applied on a noisy body volume contaminated with impulsive noise (0.1%) shown in

Figures 7d and 8d. Two projections of the morphological skeleton of the noisy body by using BMM are shown in Figures 7e and 7f. The same projections by using GFMM are shown in Figures 7g and 7h. Two projections of the spines of the body by using either BMM or GFMM are shown in Figures 8a and Figures 8b. Two projections of the spines of the noisy body by using BMM are shown in Figures 8c and 8d. The same projections by using GFMM are shown in Figures 8e and 8f. It can be observed that similar with the 2D case, the location and the shape of the morphological skeleton and spines are better preserved by using the GFMM. The BMM and GFMM skeletonization and shape decomposition were also applied on the non-convex binary volume of a tooth shown in Figures 9a and 9b. The volume was corrupted by impulsive noise (0.1%) shown in Figure 9c. Ten frames of the result of classical BMM skeletonization when applied on the original volume are shown in Figure 9d. The same ten frames of the skeleton when BMM and GFMM skeletonization are applied on the noisy volume are shown in Figures 9e and 9f respectively. It can also be observed that the location and the shape of the morphological skeleton are better preserved by using GFMM.

VI. Conclusions

In this paper, the Generalized Fuzzy Mathematical Morphology (GFMM) was proposed. It was based on a novel definition of a Fuzzy Inclusion Indicator (FII), which was defined to measure the inclusion of a fuzzy set into another, as a fuzzy set. It was proven that the FII obeys a set of axioms, which were proposed to be extensions of the known axioms that any inclusion indicator should obey, and which correspond to the desirable properties of any mathematical morphology. The proposed GFMM was compared with the classical Binary and Grayscale mathematical morphologies and it was shown that they can be considered as special cases of the GFMM. The GFMM provides a very powerful and flexible tool for morphological operations. An application for robust 2D and 3D object representation using skeletonization and shape decomposition was investigated. Extensive simulations showed that the reconstruction of noisy objects from their skeletal subsets, that can be achieved by using the GFMM is better than by using the classical BMM. Besides, the use of the GFMM for skeletonization and shape decomposition preserves the shape and the location of the skeletal subsets and spines, and therefore, can be efficiently used for object representation especially in cases of impulsive noise.

References

[1] R.M. Haralick, "Image analysis using mathematical morphology," *IEEE Trans. on Pattern Analysis and Machine Intelligence*, vol. 9, no. 4, pp. 532–550, July 1987.

[2] I. Pitas and A.N. Venetsanopoulos, *Nonlinear Digital Filters: Principles and Applications*, Kluwer Academic Publ., Boston, MA, 1990.

[3] J. Serra, *Image Analysis and Mathematical Morphology*, Academic Press, London, 1982.

[4] ed. J. Serra, *Image Analysis and Mathematical Morphology, Part II: Theoretical Advances*, Academic Press, London, 1988.

[5] J. Serra and P. Soille, *Mathematical Morphology and its Applications to Image Processing*, Kluwer Academic Publ., Boston, MA, 1994.

[6] P. Maragos, R.W. Schafer, and M. Akmal, *Mathematical Morphology and its Applications to Image and Signal Processing*, Kluwer Academic Publ., Boston, MA, 1996.

[7] P. A. Maragos and R.W. Schafer, "Morphological skeleton representation and coding of binary images," *IEEE Trans. Acoustics, Speech, and Signal Processing*, vol. 34, pp. 228–244, October 1986.

[8] I. Pitas and A.N. Venetsanopoulos, "Morphological shape decomposition," *IEEE Trans. on Pattern Analysis and Machine Intelligence*, vol. 12, no. 1, pp. 38–45, January 1990.

[9] J.M. Reinhardt and W.E. Higgins, "Comparison between the morphological skeleton and morphological shape decomposition," *IEEE Trans. on Pattern Analysis and Machine Intelligence*, vol. 18, no. 9, pp. 951–957, September 1996.

[10] J.M. Reinhardt and W.E. Higgins, "Efficient morphological shape representation," *IEEE Trans. on Image Processing*, vol. 5, no. 1, pp. 89–101, January 1996.

[11] Demin Wang, Veronique Haese-Coat, Alain Bruno, and Joseph Ronsin, "Some statistical properties of mathematical morphology," *IEEE Trans. on Signal Processing*, vol. 43, no. 8, pp. 1955–1965, August 1995.

[12] L. Koskinen, J. Astola, and Y. Neuvo, "Soft morphological filters," in *Proc. SPIE Symp. on Image Algebra and Morphological Image Processing*, 1991, vol. 1568, pp. 262–270.

[13] L. Koskinen and J. Astola, "Statistical properties of soft morphological filters," in *Proc. SPIE Symp. on Nonlinear Image Processing*, 1992, vol. 1658, pp. 25–36.

[14] F. Y. Shih and C. C. Pu, "Analysis of the properties of soft morphological filtering using threshold decomposition," *IEEE Trans. on Signal Processing*, vol. 43, no. 2, pp. 539–544, February 1995.

[15] A. T. Popov, "Convexity indicators based on fuzzy morphology," *Pattern Recognition Letters*, vol. 18, pp. 259–267, 1997.

[16] D. Sinha and E. R. Dougherty, "A general axiomatic theory of intrinsically fuzzy mathematical morphologies," *IEEE Trans. on Fuzzy Systems*, vol. 3, pp. 389–403, November 1995.

[17] I. Bloch and H. Maitre, "Fuzzy mathematical morphologies: A comparative study," *Pattern Recognition*, vol. 28, pp. 1341–1387, September 1995.

[18] A. Daneshgar, "Residuated semigroups and morphological aspects of translation invariant systems," *Fuzzy Sets and Systems*, vol. 90, pp. 69–81, 1997.

[19] S. Grossert, M. Koppen, and B. Nickolay, "A new approach to fuzzy morphology based on fuzzy integral and its application in image processing," in *Proceedings of ICPR*, Vienna, August 1996.

[20] P. D. Gader, "Fuzzy spatial relations based on fuzzy morphology," in *Proceedings of the Sixth IEEE International Conference on Fuzzy Systems*, Barcelona, July 1997.

[21] L. Zadeh, "Fuzzy sets," *IEEE Inform. and Control*, vol. 8, no. 3, pp. 338–353, 1965.

[22] L. H. Tsoukalas and R. E. Uhrig, *Fuzzy and Neural Approaches in Engineering*, Wiley, New York, 1996.

[23] A. Kaufmann and M. M. Gupta, *Introduction to Fuzzy Arithmetic: Theory and Applications*, Van Nostrand Reinhold, New York, 1985.

[24] L. Zadeh, *A Theory of Approximate Reasoning (AR)*, Memo UCB/ERL M77/58, Univ. of California, Berkeley, 1977.

[25] D. Dubois and H. Prade, *Fuzzy Sets and Systems, Theory and Applications*, Academic, Boston, 1980.

[26] G. J. Klir and B. Yuan, *Fuzzy Sets and Fuzzy Logic, Theory and Applications*, Prentice Hall, New Jersey, 1995.

[27] H. J. A. M. Heijmans, *Morphological Image Operators*, Academic, Boston, 1994.

[28] M. Werman and S. Peleg, "Min-max operators in texture analysis," *IEEE Trans. on Pattern Analysis Machine Intelligence*, vol. 7, pp. 730–733, November 1985.

[29] A. T. Popov, "Fuzzy morphology and fuzzy convexity measures," in *Proceedings of ICPR*, Vienna, August 1996.

[30] M. J. Ackerman, "The visible human project," *IEEE Proceedings*, vol. 86, pp. 504–511, March 1998.

[31] U. S. National Library of Medicine, "The visible human project," http://www.nlm.nih.gov/research/visible/visible_human.html, 1996.

Appendix A

In the following it will be proven that the fuzzy inclusion indicator proposed in (13) satisfies the axioms **A1** - **A7**. It is assumed that A, B, C, B_i are fuzzy sets. Regarding the union and intersection operators, it is assumed that the corresponding sets are defined in the same subset of the universe.

A1: $\mathbf{I}(A,B) = O$ if and only if $\forall\alpha \in [0,1], \{x : \mu_A(x) = \alpha\} \cap \{x : \mu_B(x) = 0\} \neq \emptyset$.

Proof:

$$\begin{aligned}
&\mathbf{I}(A,B) = O \Leftrightarrow \\
&\mu_{\mathbf{I}(A,B)}(u) = 0, \quad \forall u \in [0,1] \Leftrightarrow \\
&\inf_{x:\mu_A(x)=u} \mu_B(x) = 0, \quad \forall u \in [0,1] \Leftrightarrow \\
&\exists x : \mu_A(x) = u, \mu_B(x) = 0, \quad \forall u \in [0,1] \Leftrightarrow \\
&\{x : \mu_A(x) = u\} \cap \{x : \mu_B(x) = 0\} \neq \emptyset, \quad \forall u \in [0,1]
\end{aligned} \tag{A-1}$$

A2: $B \subset C \Rightarrow \mathbf{I}(A,B) \subseteq \mathbf{I}(A,C)$.

Proof: From (5) $B \subset C$ implies $\mu_B(x) \leq \mu_C(x), \forall x$. This implies that for any subset of x such that $\{x : \mu_A(x) = u\}$:

$$\begin{aligned}
&\inf_{x:\mu_A(x)=u} \mu_B(x) \leq \inf_{x:\mu_A(x)=u} \mu_C(x), \quad \forall u \in [0,1] \Rightarrow \\
&\mu_{\mathbf{I}(A,B)}(u) \leq \mu_{\mathbf{I}(A,C)}(u), \quad \forall u \in [0,1] \Rightarrow \\
&\mathbf{I}(A,B) \subseteq \mathbf{I}(A,C)
\end{aligned} \tag{A-2}$$

A3: $B \subset C \Rightarrow \mathbf{I}(C,A) \subseteq \mathbf{I}(B,A)$.

Proof: From (8) $B \subset C$ implies $B^u \subseteq C^u$, $\forall u \in [0,1]$. Let us symbolize as b_l^u and b_r^u the lower and upper limits of the classical set B^u, and similarly the limits c_l^u and c_r^u of the classical set C^u. If the fuzzy sets B, C are not convex, the α-cuts B^u, C^u can be considered as unions of i and j respectively convex sets. Then, the limits of these sets are symbolized as $b_{l_i}^u$, $b_{r_i}^u$, $c_{l_j}^u$, $c_{r_j}^u$. Since $B^u \subseteq C^u$ the following relations are valid:

$$\begin{aligned}
&\min_j\{c_{l_j}^u\} \leq b_{l_i}^u \leq b_{r_i}^u, \quad \forall i, \quad \forall u \in [0,1] \\
&\max_j\{c_{r_j}^u\} \geq b_{r_i}^u \geq b_{l_i}^u, \quad \forall i, \quad \forall u \in [0,1]
\end{aligned} \tag{A-3}$$

The above relations imply that $\inf_{x:\mu_C(x)=u} \mu_A(x) \leq \inf_{x:\mu_B(x)=u} \mu_A(x)$ and consequently that $\mathbf{I}(C, A) \subseteq \mathbf{I}(B, A)$.

A4: $\mathbf{I}(A, B) = \mathbf{I}(T(A; v), T(B; v)) \ \forall v, \qquad \mathbf{I}(A, B) = \mathbf{I}(-A, -B)$.

Proof: Equality holds since the following equalities of the membership functions are valid.

$$\mu_{\mathbf{I}(T(A;v),T(B;v))}(u) = \inf_{x:\mu_{T(A;v)}(x)=u} \mu_{T(B;v)}(x) = \inf_{(x-v):\mu_A(x-v)=u} \mu_B(x-v) = \mu_{\mathbf{I}(A,B)}(u) \quad \text{(A-4)}$$

A5: $\mathbf{I}(\bigcup_i B_i, A) = \bigcap_i \mathbf{I}(B_i, A)$.

Proof: Using (6) the relation is proven, since the following equality between the membership functions is valid:

$$\begin{aligned} &\mu_{\mathbf{I}(\cup_i B_i, A)}(u) = \inf_{x:\mu_{\cup_i B_i}(x)=u} \mu_A(x) = \inf_{\cup_i x:\mu_{B_i}(x)=u} \mu_A(x) = \\ &\inf\{\inf_{x:\mu_{B_i}(x)=u} \mu_A(x), \ \forall i\} = \inf\{\mu_{\mathbf{I}(B_i,A)}(u), \ \forall i\} \end{aligned} \quad \text{(A-5)}$$

A6: $\mathbf{I}(A, \bigcap_i B_i) = \bigcap_i \mathbf{I}(A, B_i)$.

Proof: Using (7) the relation is proven, since the following equality between the membership functions is valid:

$$\begin{aligned} &\mu_{\mathbf{I}(A,\cap_i B_i)}(u) = \inf_{x:\mu_A(x)=u} \mu_{\cap_i B_i}(x) = \inf_{x:\mu_A(x)=u} \{\min\{\mu_{B_i}(x), \ \forall i\}\} = \\ &\min\{\inf_{x:\mu_A(x)=u} \mu_{B_i}(x), \ \forall i\} = \min\{\mu_{\mathbf{I}(A,B_i)}(u), \ \forall i\} \end{aligned} \quad \text{(A-6)}$$

A7: $\mathbf{I}(A, \bigcup_i B_i) \supseteq \bigcup_i \mathbf{I}(A, B_i)$.

Proof: It should be proven that:

$$\mu_{\mathbf{I}(A,\cup_i B_i)}(u) \geq \mu_{\cup_i \mathbf{I}(A,B_i)}(u) \quad \text{(A-7)}$$

where:

$$\mu_{\mathbf{I}(A,\cup_i B_i)}(u) = \inf_{x:\mu_A(x)=u} \mu_{\cup_i B_i}(x) = \inf_{x:\mu_A(x)=u} \{\max\{\mu_{B_i}(x), \ \forall i\}\} \quad \text{(A-8)}$$

and:

$$\mu_{\cup_i \mathbf{I}(A,B_i)}(u) = \max\{\mu_{\mathbf{I}(A,B_i)}(u), \ \forall i\} = \max\{\inf_{x:\mu_A(x)=u} \mu_{B_i}(x), \ \forall i\} \quad \text{(A-9)}$$

By using (A-8) and (A-9) and classical arithmetic it can be proven that the inequality of (A-7) is valid.

List of Tables

List of Figures

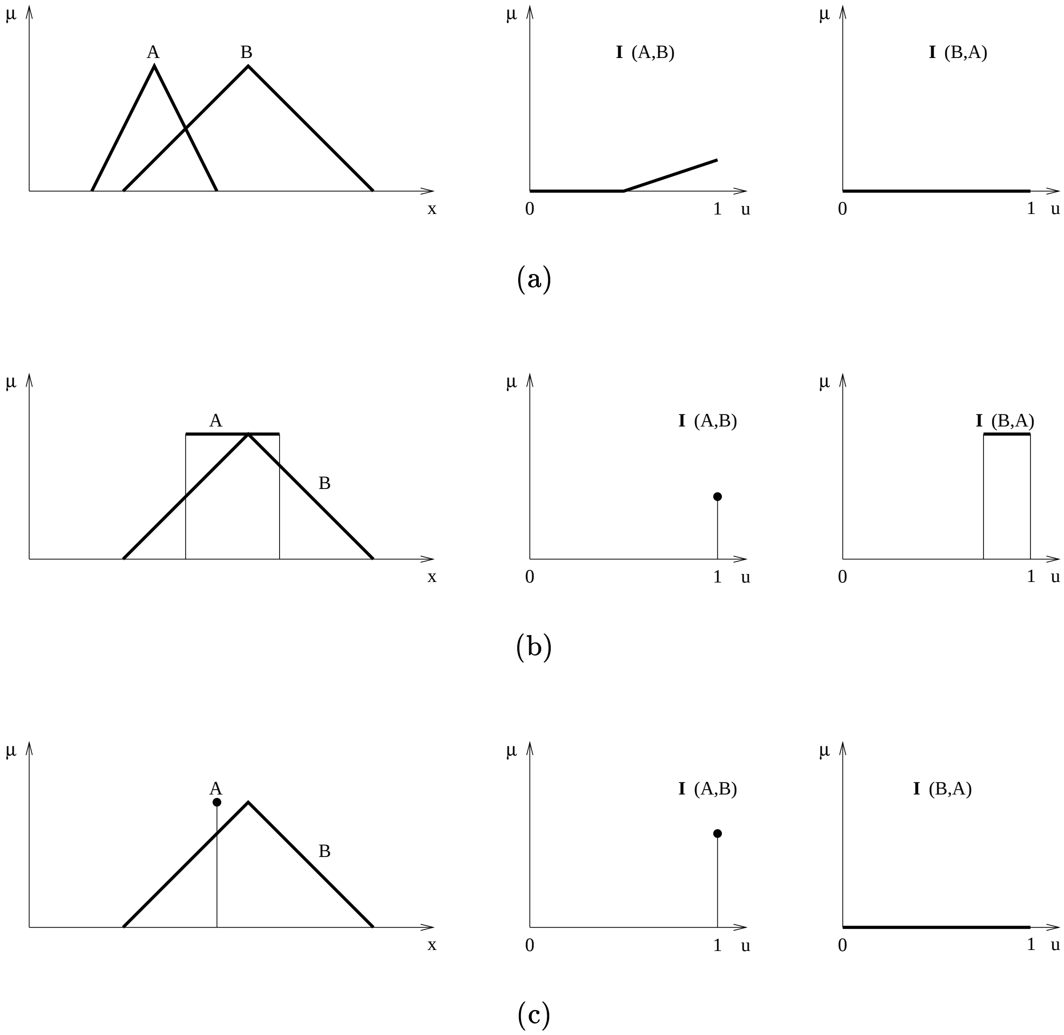

Fig. 1. Examples of fuzzy inclusion indicators, (a) of two fuzzy sets, (b) of a crisp and a fuzzy set, and (c) of a crisp value and a fuzzy set

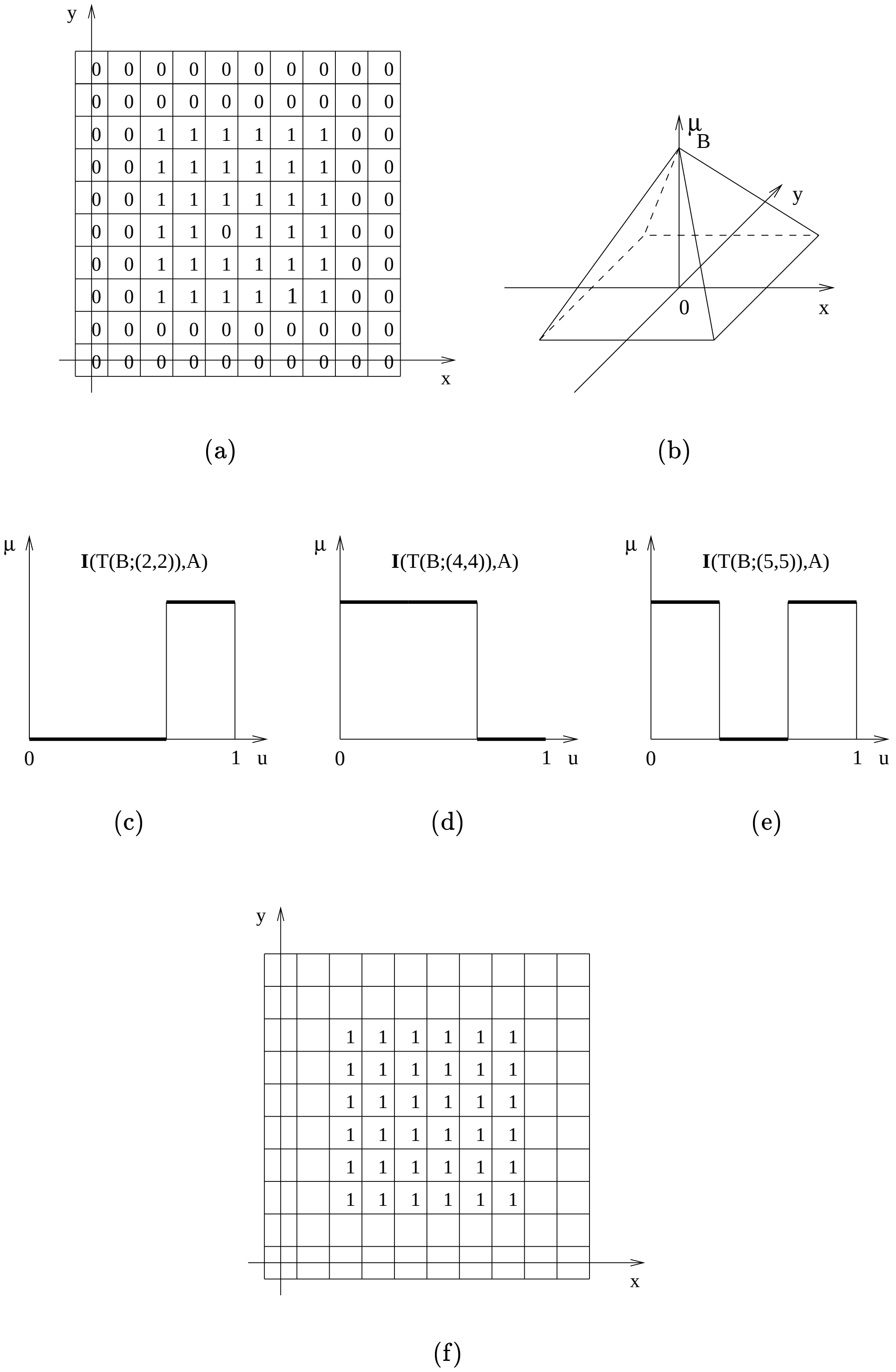

Fig. 2. An example of a fuzzy erosion operation. (a) A 10×10 binary image, (b) a 5×5 fuzzy structuring element with pyramidal fuzziness, (c), (d), (e) fuzzy inclusion indicators of the mentioned translated structuring element for various translations, and (f) the eroded image.

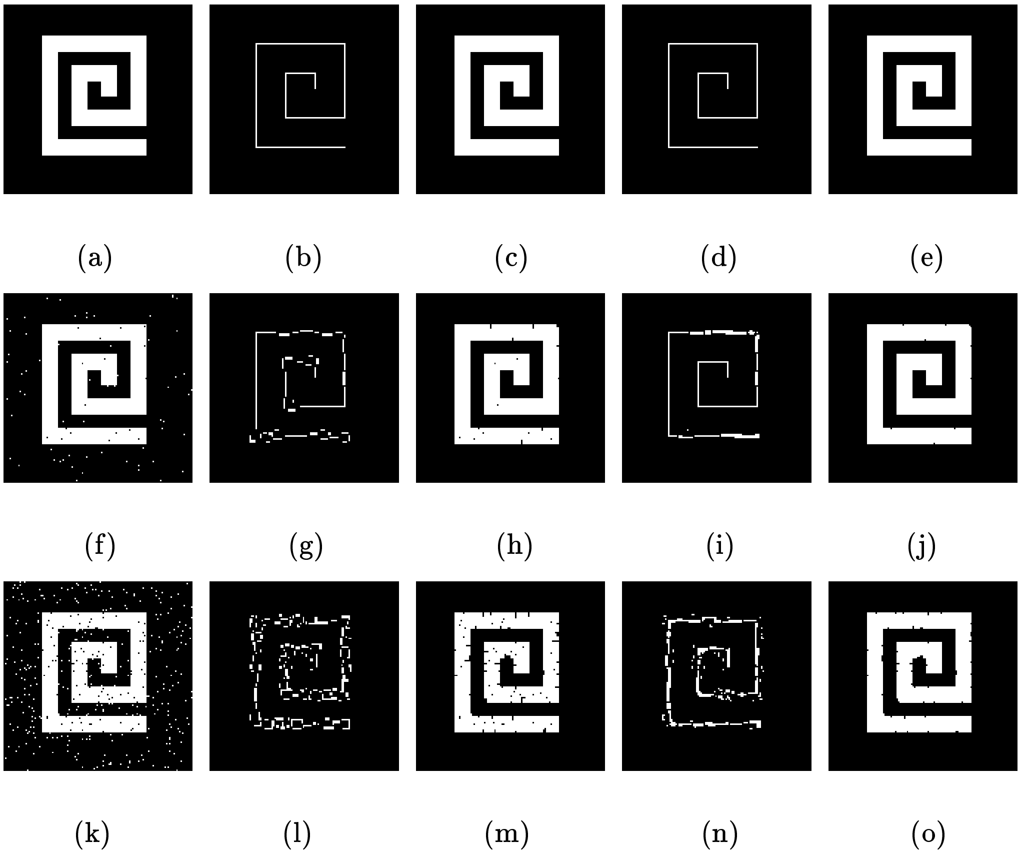

Fig. 3. (a) The original *spiral* image, (b) the BMM skeleton, (c) the reconstructed object from the BMM skeleton, (d) the GFMM skeleton, (e) the reconstructed object from the GFMM skeleton, (f) the *spiral* image contaminated with impulsive noise (1%), (g) the BMM skeleton, (h) the reconstructed object from the BMM skeleton, (i) the GFMM skeleton, (j) the reconstructed object from the GFMM skeleton, (k) the *spiral* image contaminated with impulsive noise (5%), (l) the BMM skeleton, (m) the reconstructed object from the BMM skeleton, (n) the GFMM skeleton, (o) the reconstructed object from the GFMM skeleton.

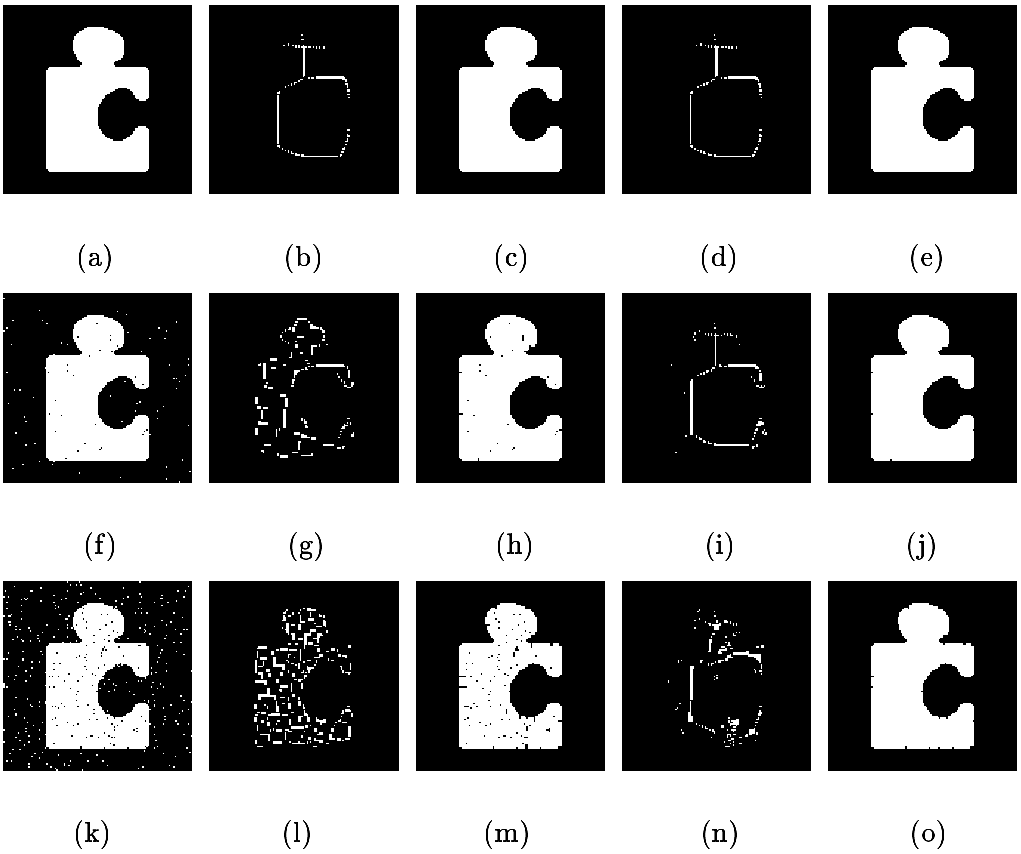

Fig. 4. (a) The original *puzzle* image, (b) the BMM skeleton, (c) the reconstructed object from the BMM skeleton, (d) the GFMM skeleton, (e) the reconstructed object from the GFMM skeleton, (f) the *puzzle* image contaminated with impulsive noise (1%), (g) the BMM skeleton, (h) the reconstructed object from the BMM skeleton, (i) the GFMM skeleton, (j) the reconstructed object from the GFMM skeleton, (k) the *puzzle* image contaminated with impulsive noise (5%), (l) the BMM skeleton, (m) the reconstructed object from the BMM skeleton, (n) the GFMM skeleton, (o) the reconstructed object from the GFMM skeleton.

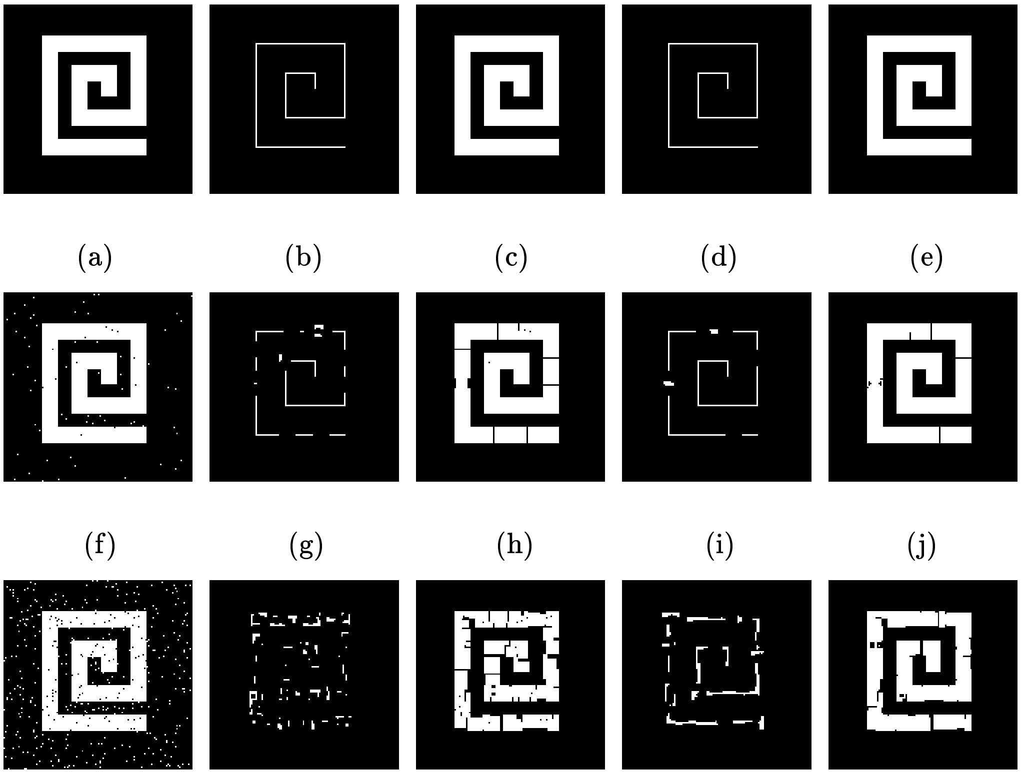

(a) (b) (c) (d) (e)

(f) (g) (h) (i) (j)

(k) (l) (m) (n) (o)

Fig. 5. (a) The original *spiral* image, (b) the BMM spines, (c) the reconstructed object from the BMM spines, (d) the GFMM spines, (e) the reconstructed object from the GFMM spines, (f) the *spiral* image contaminated with impulsive noise (1%), (g) the BMM spines, (h) the reconstructed object from the BMM spines, (i) the GFMM spines, (j) the reconstructed object from the GFMM spines, (k) the *spiral* image contaminated with impulsive noise (5%), (l) the BMM spines, (m) the reconstructed object from the BMM spines, (n) the GFMM spines, (o) the reconstructed object from the GFMM spines.

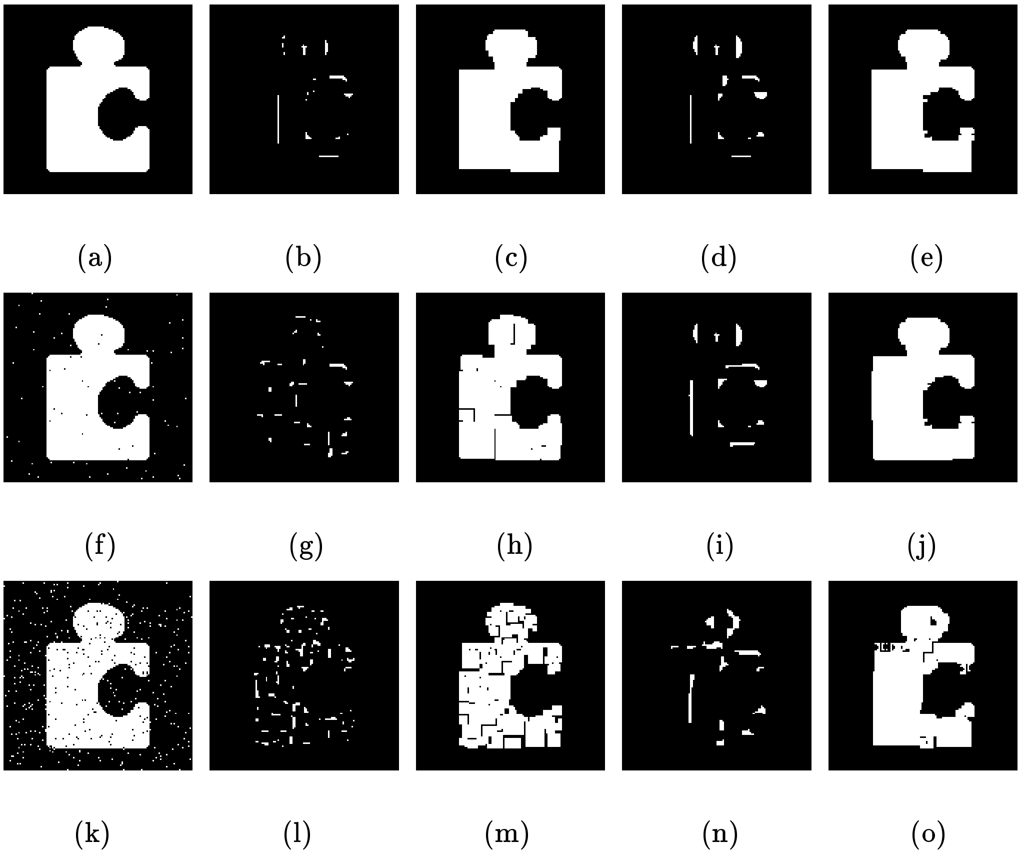

Fig. 6. (a) The original *puzzle* image, (b) the BMM spines, (c) the reconstructed object from the BMM spines, (d) the GFMM spines, (e) the reconstructed object from the GFMM spines, (f) the *puzzle* image contaminated with impulsive noise (1%), (g) the BMM spines, (h) the reconstructed object from the BMM spines, (i) the GFMM spines, (j) the reconstructed object from the GFMM spines, (k) the *puzzle* image contaminated with impulsive noise (5%), (l) the BMM spines, (m) the reconstructed object from the BMM spines, (n) the GFMM spines, (o) the reconstructed object from the GFMM spines.

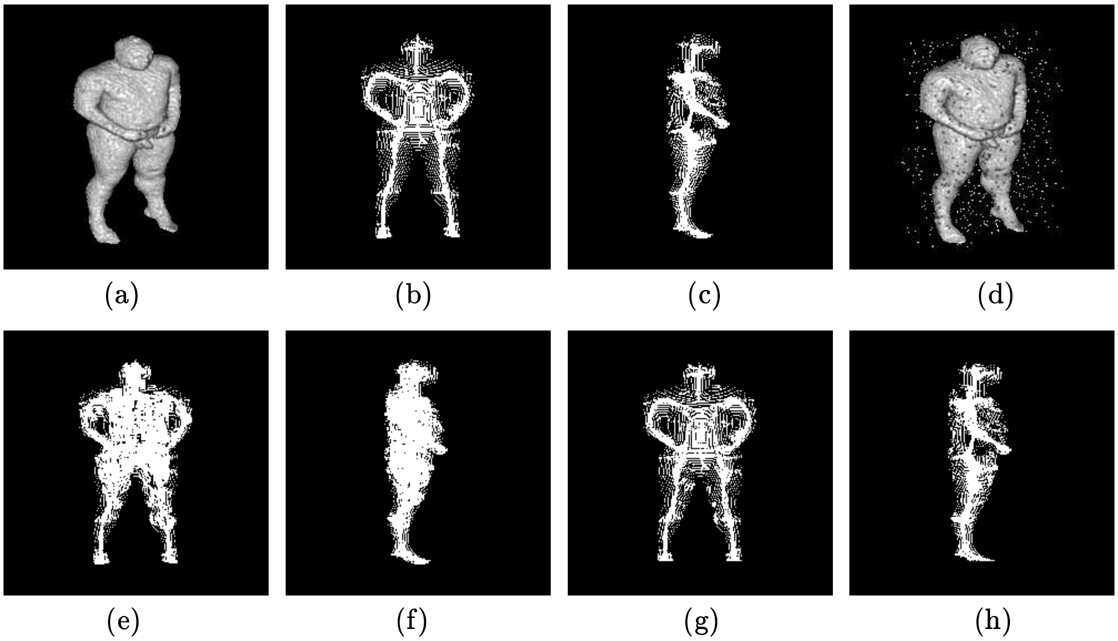

Fig. 7. (a) The original *body* volume, (b), (c) two projections of the BMM and GFMM skeleton, (d) the noisy *body* volume, (e), (f) the same projections of the BMM skeleton, (g), (h) the same projections of the GFMM skeleton.

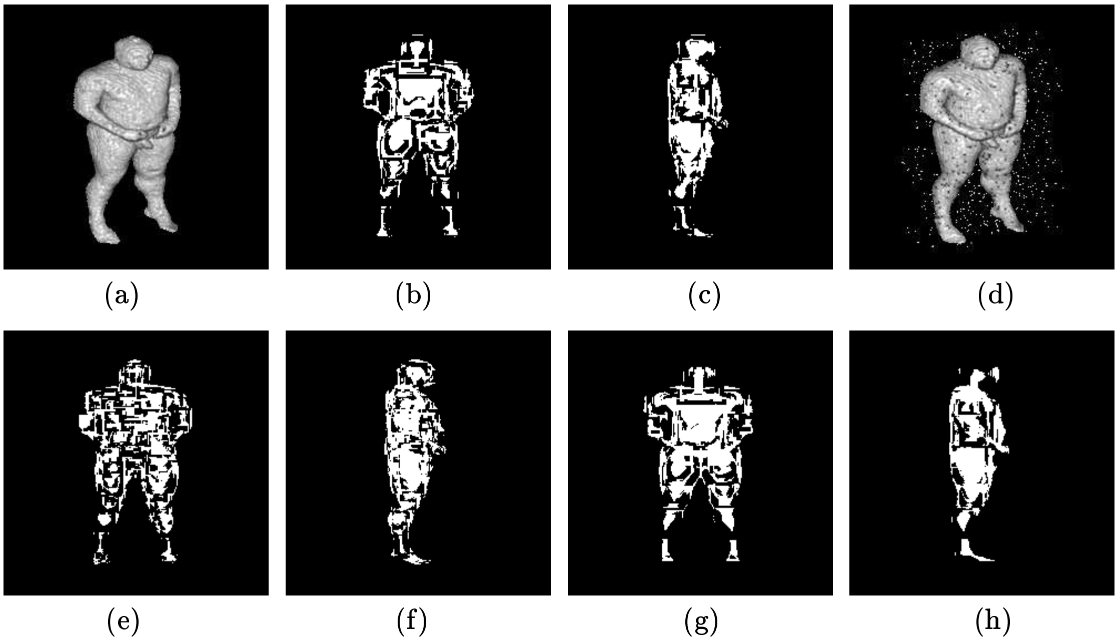

Fig. 8. (a) The original *body* volume, (b), (c) two projections of the BMM and GFMM spines, (d) the noisy *body* volume, (e), (f) the same projections of the BMM spines, (g), (h) the same projections of the GFMM spines.

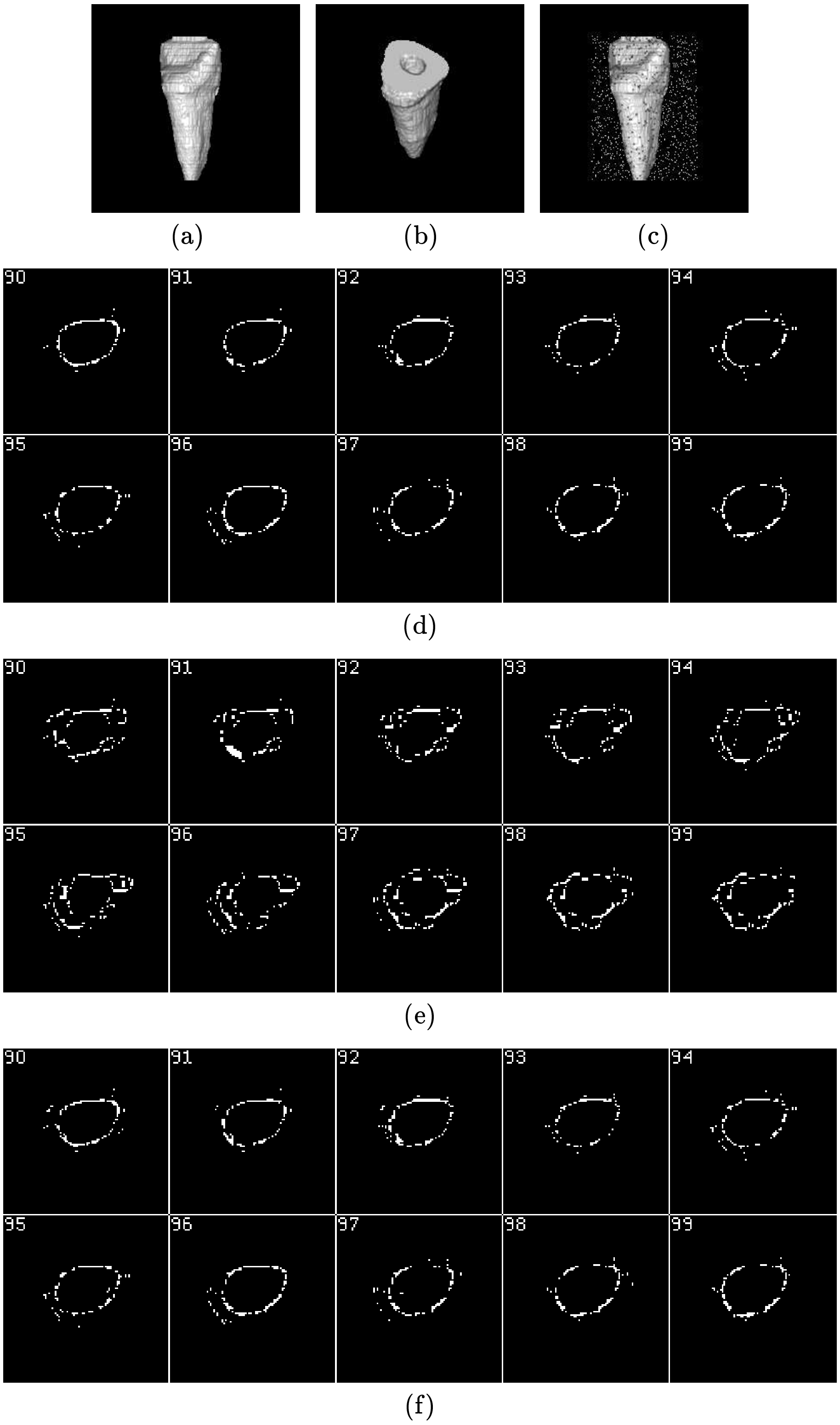

Fig. 9. (a), (b) The original *tooth* volume, (c) the noisy *tooth* volume, (d) ten frames of the original volume BMM skeleton, (e) the same frames of the noisy volume BMM skeleton, (f) the same frames of the noisy volume GFMM skeleton.

TABLE I

RESULTS FROM THE SKELETONIZATION OF THE ORIGINAL AND NOISY *spiral* IMAGES USING THE CLASSICAL BMM AND THE GFMM.

Method	Impulsive Noise (%)	Skeletal Subsets	Area of objects (% original)			Representation Error(%)		
			Noisy	Skeleton	Reconstr.	Positive	Negative	Total
BMM	0	6	100	8.83	100	0	0	0
	0.1	**6**	100.12	8.94	99.96	0.044	0	0.044
	0.2	**6**	100.21	9.19	99.85	0.145	0	0.145
	0.5	**6**	100.54	9.67	99.53	0.474	0	0.474
	1	**6**	101.13	10.15	99.25	0.754	0	0.754
	2	**6**	102.21	12.40	98.43	1.570	0	1.570
	5	**6**	105.50	16.64	95.66	4.354	0.010	4.364
	10	5.3	110.63	20.23	90.31	9.713	0.018	9.731
	20	4.1	127.15	20.42	78.11	21.937	0.047	21.984
GFMM	0	6	100	8.83	100	0	0	0
	0.1	**6**	100.12	9.00	**99.98**	0.018	0	**0.018**
	0.2	**6**	100.21	9.42	**99.94**	0.060	0	**0.060**
	0.5	**6**	100.54	9.97	**99.81**	0.186	0	**0.186**
	1	**6**	101.13	10.64	**99.70**	0.298	0	**0.298**
	2	**6**	102.21	12.11	**99.41**	0.593	0	**0.593**
	5	**6**	105.50	16.17	**98.29**	1.720	0.010	**1.730**
	10	**5.9**	110.63	22.21	**95.38**	4.636	0.018	**4.654**
	20	**5**	127.15	28.45	**85.82**	14.229	0.047	**14.276**

TABLE II

RESULTS FROM THE SKELETONIZATION OF THE ORIGINAL AND NOISY *puzzle* IMAGES USING THE CLASSICAL BMM AND THE GFMM.

Method	Impulsive Noise (%)	Skeletal Subsets	Area of objects (% original)			Representation Error(%)		
			Noisy	Skeleton	Reconstr.	Positive	Negative	Total
BMM	0	18	100	4.69	100	0	0	0
	0.1	17.9	100.07	5.27	99.93	0.073	0	0.073
	0.2	17.8	100.14	5.84	99.84	0.160	0.002	0.162
	0.5	14.9	100.35	7.37	99.62	0.388	0.004	0.039
	1	13.4	100.68	9.22	99.28	0.729	0.010	0.074
	2	11.8	101.36	12.27	98.55	1.469	0.014	1.484
	5	7.2	103.39	17.04	96.30	3.728	0.025	3.753
	10	5.8	106.62	20.33	91.38	8.697	0.075	8.771
	20	4.4	112.66	21.60	80.06	19.988	0.052	20.039
GFMM	0	18	100	4.69	100	0	0	0
	0.1	**18**	100.07	4.69	**99.97**	0.029	0	**0.029**
	0.2	**18**	100.14	4.84	**99.94**	0.062	0.002	**0.064**
	0.5	**18**	100.35	4.95	**99.88**	0.129	0.004	**0.133**
	1	**17.7**	100.68	5.46	**99.80**	0.214	0.010	**0.224**
	2	**17.8**	101.36	5.70	**99.56**	0.457	0.015	**0.471**
	5	**16.2**	103.39	9.43	**98.90**	1.125	0.025	**1.150**
	10	**10.5**	106.62	20.70	**97.02**	3.051	0.075	**3.126**
	20	**5.7**	112.66	30.66	**89.80**	10.247	0.048	**10.295**

TABLE III

Results from the Shape Decomposition of the original and noisy *spiral* images using the classical BMM and the GFMM.

Method	Impulsive Noise (%)	Spines	Area of objects (% original)			Representation Error(%)		
			Noisy	Spines	Reconstr.	Positive	Negative	Total
BMM	0	1	100	8.83	100	0	0	0
	0.1	1.3	100.12	8.44	99.66	0.342	0	0.342
	0.2	2	100.21	7.89	99.03	0.966	0	0.966
	0.5	3.4	100.54	6.99	97.77	2.227	0	2.227
	1	4.4	101.13	6.43	96.71	3.289	0	3.289
	2	5	102.21	6.91	94.27	5.734	0	5.734
	5	5	105.50	9.27	88.21	11.800	0.005	11.805
	10	4.3	110.63	11.83	**81.72**	18.285	0.010	**18.296**
	20	**3.1**	127.15	14.12	**70.97**	29.057	0.026	**29.083**
GFMM	0	1	100	8.83	100	0	0	0
	0.1	**1.1**	100.12	8.61	**99.71**	0.285	0	**0.285**
	0.2	**1.7**	100.21	8.45	**99.17**	0.826	0	**0.826**
	0.5	**2.2**	100.54	8.08	**98.17**	1.834	0	**1.834**
	1	**2.9**	101.13	7.66	**96.87**	3.131	0	**3.131**
	2	**3.5**	102.21	7.97	**95.08**	4.924	0	**4.924**
	5	**4.1**	105.50	11.36	**89.15**	10.857	0.003	**10.860**
	10	**4.2**	110.63	14.87	80.04	19.956	0	19.956
	20	3.4	127.15	19.69	67.87	32.139	0.013	32.152

TABLE IV

RESULTS FROM THE SHAPE DECOMPOSITION OF THE ORIGINAL AND NOISY *puzzle* IMAGES USING THE CLASSICAL BMM AND THE GFMM.

Method	Impulsive Noise (%)	Spines	Area of objects (% original)			Representation Error(%)		
			Noisy	Spines	Reconstr.	Positive	Negative	Total
BMM	0	6	100	2.97	**94.75**	5.251	0	**5.251**
	0.1	7.1	100.07	3.58	**95.13**	4.867	0	**4.867**
	0.2	8	100.14	3.83	**95.16**	4.840	0.002	**4.842**
	0.5	8.7	100.35	4.61	**95.01**	4.988	0	**4.988**
	1	9.1	100.68	4.81	93.65	6.355	0.004	6.359
	2	8.4	101.36	6.25	92.25	7.763	0.010	7.773
	5	6.1	103.39	8.59	87.58	12.437	0.019	12.455
	10	4.8	106.62	11.07	**81.70**	18.352	0.048	**18.400**
	20	3.4	112.66	13.63	**71.42**	28.614	0.035	**28.649**
GFMM	0	6	100	5.25	94.38	5.625	0	5.625
	0.1	**6.2**	100.07	5.06	94.25	5.745	0	5.745
	0.2	**6.3**	100.14	5.35	94.49	5.515	0	5.515
	0.5	**6.3**	100.35	5.35	94.41	5.594	0	5.594
	1	**6.1**	100.68	5.93	**94.86**	5.143	0.006	**5.149**
	2	**5.5**	101.36	6.87	**94.13**	5.880	0.010	**5.890**
	5	**6.5**	103.39	8.39	**89.76**	10.257	0.012	**10.270**
	10	**6.6**	106.62	12.75	80.94	19.089	0.029	19.118
	20	**3.9**	112.66	19.72	71.16	28.871	0.027	28.898